



Development of an extensive database of mechanical and physical properties for reduced-activation martensitic steel F82H

S. Jitsukawa ^{a,*}, M. Tamura ^b, B. van der Schaaf ^c, R.L. Klueh ^d, A. Alamo ^e,
C. Petersen ^f, M. Schirra ^f, P. Spaetig ^g, G.R. Odette ^h, A.A. Tavassoli ^e,
K. Shiba ^a, A. Kohyama ⁱ, A. Kimura ⁱ

^a *Radiation Effects and Analyses, Department of Materials Science, JAERI, 2-4 Shirakata, Tokai-Mura, Ibaraki-Ken 319-1195, Japan*

^b *Defense Academy, Yokosuka-Shi, Kanagawa-Ken 239-0811, Japan*

^c *NRG, Postbox 25, Petten, The Netherlands*

^d *ORNL, Oak Ridge, TN 37831, USA*

^e *CEA/Saclay, 91191 Gif sur Yvette cedex, France*

^f *FZK-IMF, Postfach 3640, Karlsruhe, Germany*

^g *PSI, Villigen, Switzerland*

^h *UCSB, CA 93106-5070, USA*

ⁱ *IAE, Kyoto University, Gokasho, Uji, Kyoto 611-0011, Japan*

Abstract

Tensile, fracture toughness, creep and fatigue properties and microstructural studies of the reduced-activation martensitic steel F82H (8Cr–2W–0.04Ta–0.1C) before and after irradiation are reported. The design concept used for the development of this alloy is also introduced. A large number of collaborative test results including those generated under the International Energy Agency (IEA) implementing agreements are collected and are used to evaluate the feasibility of using reduced-activation martensitic steels for fusion reactor structural materials, with F82H as one of the reference alloys. All the specimens used in these tests were prepared from plates obtained from 5-ton heats of F82H supplied to all participating laboratories by JAERI. Many of the results have been entered into relational databases with emphasis on traceability of records on how the specimens were prepared from plates and ingots.

© 2002 Published by Elsevier Science B.V.

1. Introduction

It has long been recognized that ferritic/martensitic steels have inherently good dimensional stability under intense irradiation conditions, and the chemical composition of such steels is suitable for commercial production of a reduced-activation composition without a large industrial investment. The first steels considered for fusion

were the Cr–Mo steels (e.g., modified 9Cr–1Mo steel). Because of long radioactive decay times for some of the activated species in these steels (e.g., molybdenum and niobium), reduced-activation ferritic/martensitic (RAF/M) steels were developed in the 1980s in the EU, Japan and the US by substituting tungsten and vanadium for the alloying elements molybdenum and niobium. In the 1990s, the Annex II working group (WG) under the auspices of the International Energy Agency (IEA) for the fusion reactor materials development decided to promote an international collaboration to accelerate the determination of the feasibility of the RAF/M steels as blanket structural materials for fusion reactors.

* Corresponding author. Tel.: +81-29 282 5391; fax: +81-29 282 5922.

E-mail address: jitsukawa@ifmif.tokai.jaeri.go.jp (S. Jitsukawa).

2. IEA RAF/M steel working group

Nine workshops have been held by the IEA RAF/M steel WG through 2000, and nine proceedings in addition to several reports have been published [1–6]. This paper is a review of the collaborative test program based on those reports and other publications that have been generated on the work.

At the first WG meeting in 1992, it was agreed that the feasibility of the use of F/M steels for fusion must be established, and that process could be accelerated by international collaboration.

F82H had been developed by JAERI and NKK corporation. In 1992 and 1993, the IEA WG reviewed the specifications of F82H and approved an F82H composition as one of the alloys for the collaborative test program (later, JLF1, developed by Japanese universities, and EUROFER, developed by EU institutes, were also approved). JAERI and NKK then prepared a 5-ton ingot of the IEA heat of F82H (IEA-F82H), taking care to reduce the residual Nb level to about 1 wppm or less using high-purity iron and chromium (the maximum allowable level of Nb for a ‘reduced activation’ alloy is of the order of 1 wppm [1,7]). A second 5-ton heat was subsequently produced to allow the fabrication of TIG-welded plates that were made part of the international collaboration between the EU, Japan, and the US.

Test plans developed by the WG and subsequently carried out included the following general test items: chemical analysis of the heats including the precise analysis of the residual level of Mo and Nb, measurement of physical properties, examination of the microstructural response to heat treatment, and mechanical tests before and after irradiation. In addition, the methodology to evaluate the failure criteria of structures with RAF/M steels has been delineated. This task included the evaluation of specimen size effects on fracture toughness values. Compilation of a database has been carried out in both the EU and Japan so that knowledge from the collaborative program can be shared by all WG members.

Table 1
Chemical composition (wt%) and heat treatment condition for IEA-F82H

Fe	C	Si	Mn	Cr	V	W	N	Ta
Base	0.09	0.10	0.21	7.46	0.15	1.96	0.006	0.023
	JAERI	FZK						
Nb (wppm)	1	2.5 ± 1						
Mo (wppm)	30	46 ± 17						

Normalization: 1040 °C × 40 min, air cooled; tempering: 740 °C × 1 h.

Analysis method – JAERI: mass spectrometry and FZK: activation analysis.

3. Alloy design

Past experience with F/M steels containing 2.25–12% Cr indicates that alloys containing around 9% Cr exhibit higher strength at elevated temperatures and have microstructures that are easily controlled by heat treatment to optimize their mechanical properties. F82H was planned as a reduced-activation modification of the 9Cr–1MoNbV steel (modified 9Cr–1Mo), keeping the mechanical properties within similar levels without changing heat treatment specifications. One of the advantages of this strategy of making minor changes to a code-approved material is that it may result in an easier and more rapid qualification of the new alloy. This may also encourage the use of the alloy in the core components of fast breeder reactors and to those of the fusion experimental reactor ITER.

4. Chemical composition and the feasibility of reduced activation heat production

Results of the chemical analysis of one of the 5-ton IEA heats of F82H is listed in Table 1. The heat was produced with high-purity raw materials using a 5-ton commercial vacuum induction furnace [7]. Residual impurity levels of Mo and Nb were examined to evaluate the feasibility of obtaining products with low enough impurity levels to qualify as ‘reduced activation’. Because the requirement for Nb is quite severe, care was taken to minimize Nb levels, and levels obtained in analyses by both NKK and FZK Karlsruhe were of the order of 1 wppm. This suggests the feasibility of reduced-activation steel production using facilities available for the commercial production of steels.

5. Unirradiated properties

5.1. Microstructure and the effect of heat treatment

The standard heat treatment for IEA-F82H was austenitization for 0.5 h at 1040 °C followed by an air cool

(normalization treatment); it was then tempered for 1 h at 740 °C. The microstructure after normalization was 100% martensite. No delta ferrite was detected by either optical or electron microscopy.

Hardness was measured after tempering for 2 h at temperatures ranging from 300 to 850 °C [8,9]. At temperatures above 550 °C, hardness decreased with temperature up to around 800 °C (the A_{c1b} temperature was estimated to be 835 °C). The A_{c1b} , A_{c1c} , M_s and M_f temperatures were determined by hardness testing, thermal expansion measurement and optical microscopy. They are 835, 915, 425 and 220 °C, respectively [9]. The average diameter of prior austenite grains was about 90 μm , corresponding to an ASTM standard average grain size of No. 4.

5.2. Physical properties

The first wall of the blanket of a fusion reactor will be exposed to a high heat flux from the plasma, causing a thermo-mechanical loading on the first wall structural material. Also, the ferromagnetism of the structural material is thought to induce a mechanical loading by an electro-magnetic force and to produce an error field affecting plasma control.

The thermal expansion coefficient and the thermal conductivity at 400 °C were evaluated to be $11.5 \times 10^{-6} \text{ K}^{-1}$ and 32.5 W/m K, respectively. The saturation level of the magnetic flux was 20 000 G at an ambient temperature. This was gradually decreased with temperature to 17 000 G at 400 °C. These and most of the other physical properties are similar to those of modified 9Cr–1Mo steel.

The WG reviewed the research on the effects of ferromagnetism (summarized by Klueh) [5]. The review indicated that the electro-magnetic force on the blanket and the effect of the error field on the plasma control were in the manageable range.

5.3. Mechanical properties

5.3.1. Tensile properties

Yield stress levels of the F82H base metal are shown as functions of temperature in Fig. 1 [9] along with results for MANET II (a conventional Cr–Mo steel). Tests for F82H have been carried out by five organizations in the EU and Japan (CEA, CIEMAT, ECN, FZK and JAERI). The scatter of the plots was not only the result of the inhomogeneity of the heat of steel but also the result of the difference of the test methods between the organizations. At temperatures above 500 °C, the yield stress level decreased rapidly with temperature. The stress level for IEA-F82H was similar to that for MANET-II in this temperature range, although IEA-F82H exhibited smaller stress levels at temperatures below 400 °C. Yield stress levels of several products (plates and

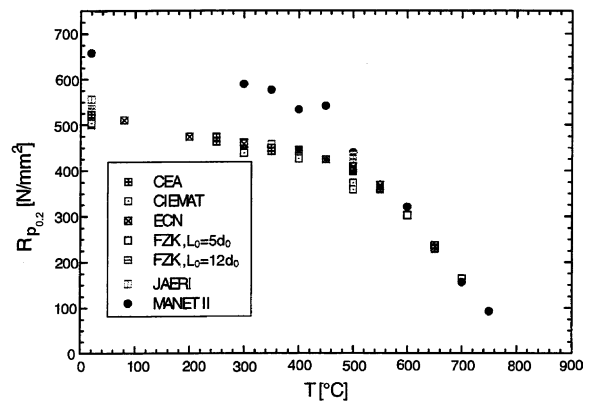


Fig. 1. Temperature dependence of the yield stress for IEA-F82H performed by five organizations [9].

tubes) of modified 9Cr–1Mo steel found in the literature and that of F82H were similar at all temperatures examined [10]. Scatter for the modified 9Cr–1Mo was larger than that for F82H. This possibly resulted from the difference in thermo-mechanical treatments of the different product forms of the modified 9Cr–1Mo steel. On the other hand, the smaller scatter for the results of IEA-F82H suggests that there may not be a significant problem in producing a homogeneous product of F82H, although yield strength is not very sensitive to inhomogeneity.

5.3.2. Impact properties

Impact energies are plotted against test temperatures in Fig. 2 [9]. KLST impact specimens with cross section of $3 \times 4 \text{ mm}$ were used for the tests conducted by six organizations in the EU (CEA, CRPP, ECN, ENEA, FZK and VTT). The ductile–brittle transition temperature (DBTT) was evaluated to be about -60 °C . In tests at JAERI using standard Charpy-V-notch (CVN) specimens, it was evaluated to be -50 °C . In comparison with the values for non-reduced-activation heats, the transition temperature for the F82H was relatively low.

The DBTT tends to be affected by inhomogeneity of the heat. However, the rather small scatter again indicates good homogeneity of the IEA-F82H.

5.3.3. Fracture toughness

The temperature dependence of the fracture toughness was obtained from 0.4T-CT (10 mm thickness) specimens [5]. A fracture toughness value of $350 \text{ MPa m}^{1/2}$ (obtained by J_Q tests) at 20 °C is fairly large. It appears that the DBTT by this method is between -50 and 0 °C.

Mixed mode fracture toughness at an ambient temperature was also evaluated as a function of the minimum angle between crack plane and the loading direction [2]. Mixed mode fracture toughness of mode I

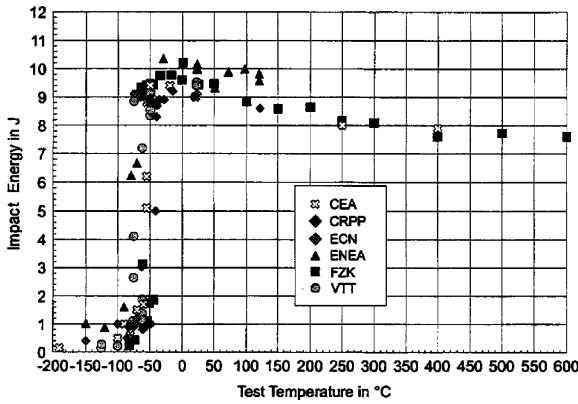


Fig. 2. Temperature dependence of impact energy for IEA-F82H [9]. Tests were performed by six organizations using KLST type miniaturized impact specimens.

and mode III loading became minimal at an angle of 45°. The value was about half of that of mode I loading.

5.3.4. Creep properties

Larson–Miller diagrams for the results of creep rupture tests are plotted in Fig. 3 [4]. Results for modified 9Cr–1Mo steel obtained by CEA are also plotted (smaller symbols) in the figure. The results indicate that the creep strength of IEA-F82H was similar to that of modified 9Cr–1Mo steel.

5.3.5. Fatigue property

Because of the large heat flux from the plasma in a fusion reactor, thermal fatigue is thought to be a critical failure mode for the first wall of the blanket.

Fig. 4 shows the relationship between the strain amplitude and the number of cycles to failure from constant strain amplitude fatigue tests at temperatures

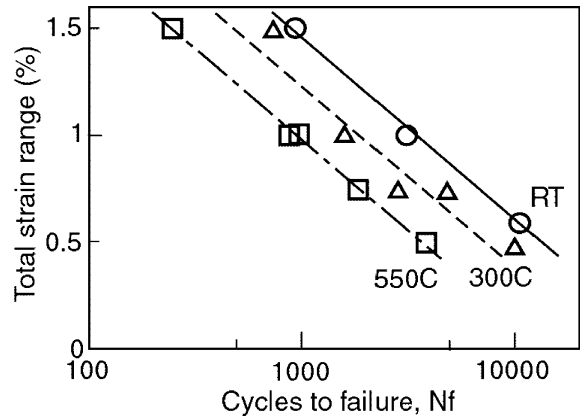


Fig. 4. Strain amplitude–number of cycles to failure relations for IEA-F82H [5].

of ambient, 300 and 550 °C [5]. The fatigue life is similar to or slightly shorter than that of modified 9Cr–1Mo steel [10].

Thermal fatigue tests using hollow cylindrical specimens have also been carried out by several organizations. The results for IEA-F82H, MANET II and OPTIFER were obtained between 200 and 650 °C [9]. Thermal fatigue life did not appear to be strongly dependent on the steel composition.

5.4. Compatibility

Corrosion rates in high-temperature pressurized water containing a dissolved oxygen level of 0.8 ppm at temperatures of around 220 to 300 °C were obtained [4]. Those for HT9 were also obtained. Below 260 °C, a weight loss occurred; however, there was a weight gain above 260 °C. The weight change for IEA-F82H was

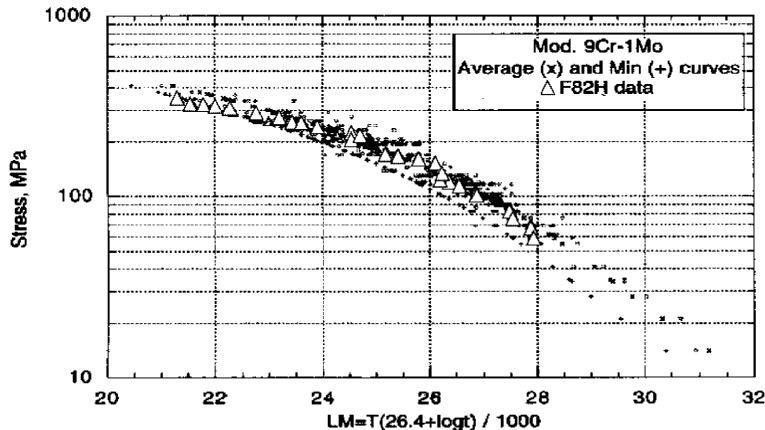


Fig. 3. Larson–Miller plots for the creep rupture test results of IEA-F82H [4]. The creep strength of IEA-F82H was similar to that of modified 9Cr–1Mo steel.

equal to or smaller than that of HT9. This suggests that the compatibility of IEA-F82H with water may not be a major issue. Because of the scarce data, however, it is not possible to make a clear recommendation for water condition during service.

The compatibilities of F82H with ceramic breeding materials and with neutron multiplier materials are also important subjects to be evaluated. However, studies of F82H with these materials have not yet been conducted. It has been reported that MANET II exhibits better compatibility with those materials than 316 stainless steel. This suggests that the compatibility of F82H with those materials will be comparable to or better than the compatibility of those materials with 316 stainless steel.

6. Properties after irradiation

6.1. Mechanical properties

6.1.1. Tensile properties

Dose dependence of yield stress for several ferritic/martensitic steels after irradiation at 325 °C in the Osiris reactor is shown in Fig. 5 [4]. Reduced-activation alloys of IEA-F82H and LA12LC exhibited smaller irradiation hardening compared to those of the MANET steels. This suggests a smaller toughness degradation by irradiation for reduced-activation alloys.

Dose dependence of the tensile test results for IEA-F82H irradiated in HFIR at 200–500 °C is shown in Fig. 6 [6]. Test temperatures were at or near the irradiation temperatures. Below 400 °C, yield stress increased linearly with the logarithm of the displacement damage levels to above 10 dpa. Elongations decreased with dose, and at temperatures of 400 and 500 °C, the change caused by irradiation was rather small.

Post-irradiation tensile tests at an ambient temperature were also performed for base metal, weld metal, and

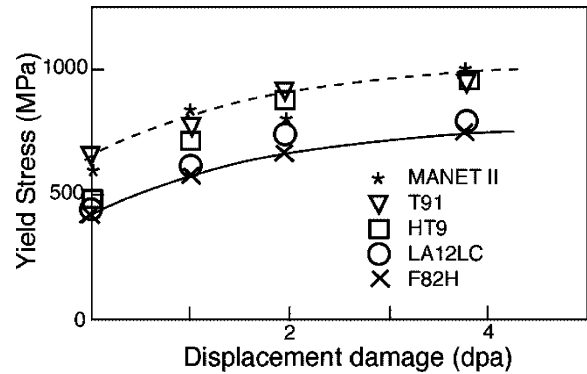


Fig. 5. Dose dependence of yield stress for IEA-F82H [4]. Irradiation was performed in the Osiris reactor. Reduced-activation steels F82H and LA12LC hardened less than the non-reduced-activation steels.

weld joint specimens irradiated to 5 dpa at 300 °C in HFIR. Welding (TIG) was carried out with a filler wire of 0.08C–7.7Cr–2W–0.2V–0.02Ta for plates with a thickness of 15 mm. The temperature and the time of the post-weld heat treatment were 720 °C and 1 h, respectively. The weld and the base metals hardened more by irradiation than the weld joint. This suggests that a region with smaller irradiation hardening was produced in the heat affected zone, although the unirradiated properties for these specimens were rather similar. This may imply that heat treatment may be used to reduce the irradiation-induced DBTT shift and toughness degradation, which are closely related to irradiation hardening.

6.1.2. Impact properties

It is well known that the DBTT shift in RAF/M steels caused by irradiation often becomes quite large, and this is recognized to be one of the key issues for ferritic/

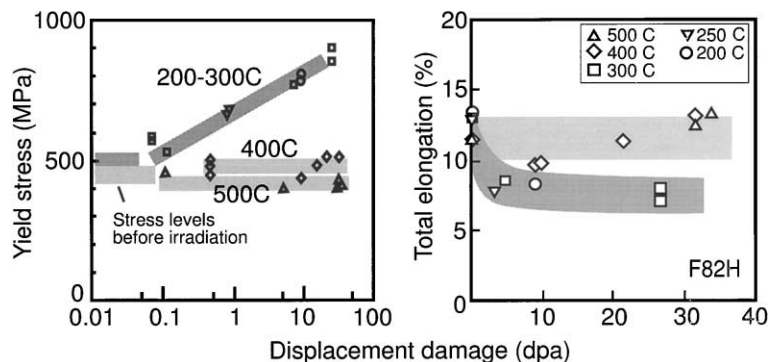


Fig. 6. Dose dependence of (a) yield stress and (b) total elongation of IEA-F82H irradiated in HFIR to about 20 dpa [6]. The yield stress level increased linearly with the logarithm of the damage level with no hardening observed at temperatures of 400 and 500 °C. Total elongation decreased with dose at temperature below 400 °C.

martensitic steels [11,12]. The DBTT for several ferritic/martensitic steels after irradiation in HFR at 300 °C is plotted in Fig. 7 as functions of dose [9]. Impact specimens of the KLST type were used. The DBTT shift for the reduced-activation steels OPTIFER, ORNL 9Cr–2WVTa and IEA-F82H were smaller than that for non-reduced-activation steels MANET I and II, suggesting a better performance of the reduced-activation steels.

6.1.3. Fracture toughness

Miniaturized DCT specimens 4.6 mm thick were irradiated in HFIR to 3.8 dpa at temperatures ranging from 221 to 405 °C. Fracture toughness values are plotted against test temperatures in Fig. 8 [6]. For the specimens irradiated above 310 °C, degradation of fracture toughness and the DBTT shift by irradiation were rather small. However, a large DBTT shift of 155 °C was obtained for the specimens irradiated below 300 °C. The solid lines in the figure were determined by the master curve method.

6.2. Swelling

It has been reported that voids were observed to form in boron-doped F82H irradiated to about 50 dpa in HFIR [13,14]. Swelling reached almost 1% in one of the specimens, although the void distribution was not homogeneous. It was also reported that swelling increased with helium (He) and hydrogen levels in specimens irradiated in a multi-ion-beam irradiation facility [15]. However, swelling was successfully suppressed by introducing a higher dislocation density by cold working [15,16].

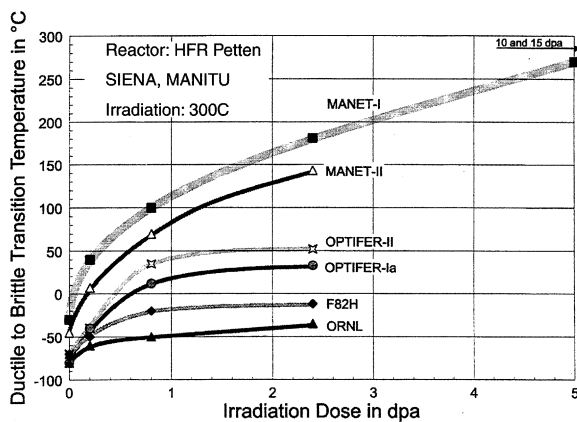


Fig. 7. Dose dependence of DBTT of IEA-F82H irradiated in HFR [9]. Results for the reduced-activation steels OPTIFER and ORNL 9Cr–2WVTa and the non-reduced-activation steels MANET I and II are also plotted. The DBTT shifts of the reduced-activation steels were smaller than for MANET I and II.

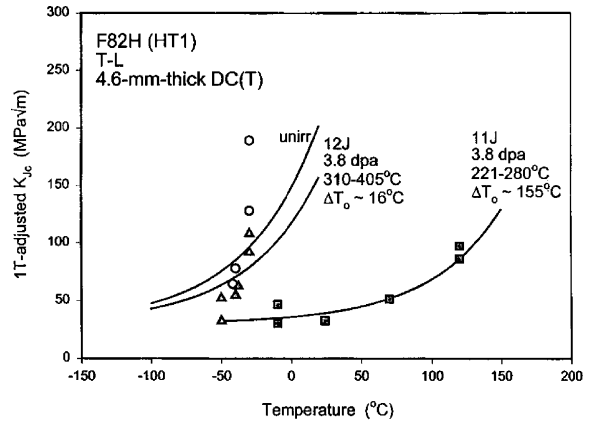


Fig. 8. Temperature dependence of K_{IC} fracture toughness values of IEA-F82H before and after irradiation in HFIR [6]. The DBTT shift was large for specimens irradiated below 300 °C.

7. Database and the quality control of the data

Results obtained in the IEA collaboration were compiled in databases in the EU and Japan [3–6]. These databases document not only the data, but they also indicate the type of specimen used, the location of the specimen in the plate it was taken from, the plate–ingot relation, and the history of thermo-mechanical treatment of the plate used, as illustrated in Fig. 9. This type of specification is beneficial to ensure the reliability of the data, and it reflects the experience gained in establishing databases for the European FBR program and ITER, in addition to that of the database for the collaborative irradiation program between JAERI and ORNL.

An image of the input page used in the Japanese database is shown in Fig. 10. Examples of the properties available in the databases are listed in Table 2.

8. Method to evaluate fracture criteria of the structure and the effects of specimen size and configuration

The fracture condition of a ferritic/martensitic steel structure is often controlled by the fracture toughness and the configuration of the structure, in addition to the size and the location of the flaw. Because the irradiation volume in a research reactor is limited, miniaturized specimens tend to be used for irradiation experiments. On the other hand, crack size and the constraint factor at the crack front depend on the flaw location and the dimension of the structure. To reduce the errors caused by these limitations, a ‘master curve’ method has been shown to be useful [3–6]. Contribution to this activity has been made mostly from the US participants. One of

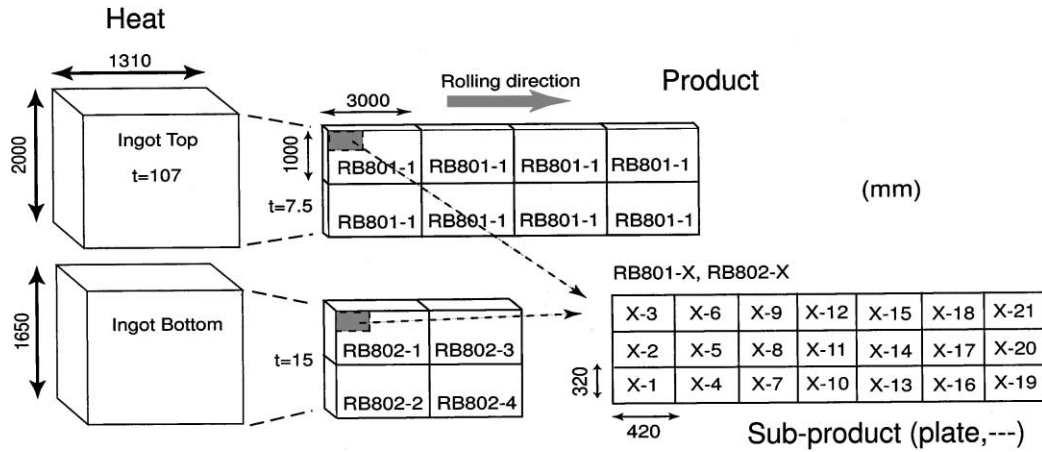


Fig. 9. An example of the items recorded in the database to ensure the reliability of the data (heat, product, sub-product and specimen).

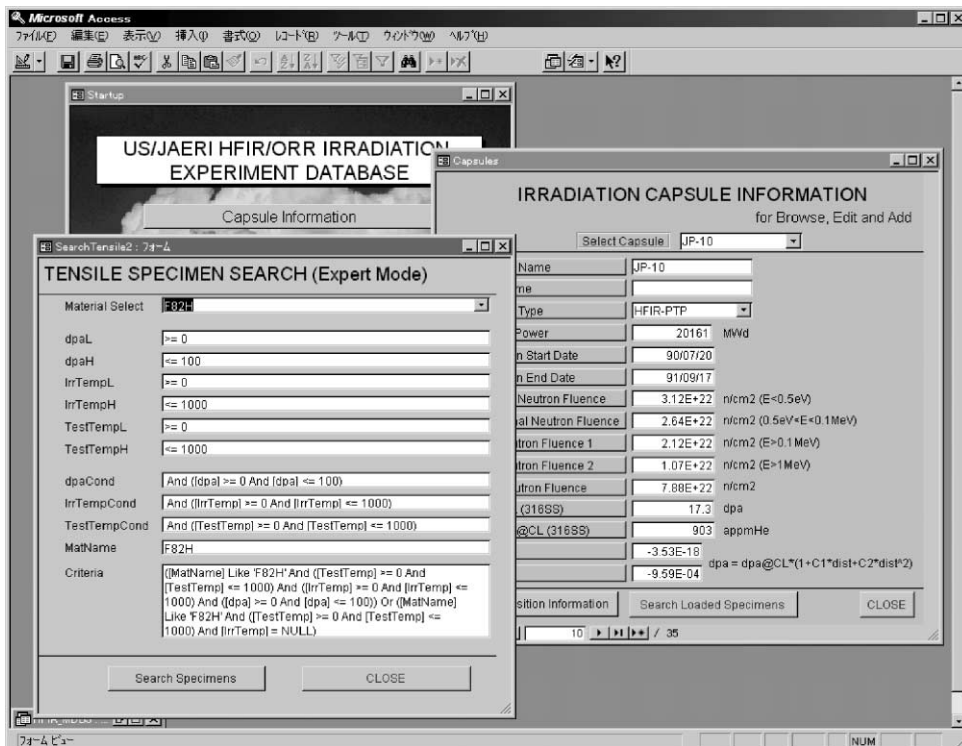


Fig. 10. Images of the input page for the Japanese database [6].

Table 2
Example of the properties compiled in the databases

Tensile	Creep	Fatigue	Impact
Yield strength, ultimate strength, uniform elongation (STN), reduction of area	Creep curves, creep ductility, time to stress rupture, time to 1% strain	Number of cycles to failure, stress amplitude, strain amplitude, cyclic stress-strain relation	Specimens: CVN, 1/2CVN, KLST, 1/3CVN

the outcomes of this activity is the ability to calculate the effect of size and constraint on fracture toughness. Results indicate a range of bend specimen sizes with a/W (ratio between crack length and specimen width) ~ 0.5 to obtain a single ‘master curve’ [5].

9. Summary and future work

Mechanical properties of the IEA-F82H with and without irradiation were equal to or slightly superior to modified 9Cr–1Mo steel. Compatibility of the IEA-F82H with high-temperature water was equal to or slightly superior to HT9. Thermo-physical properties of the IEA-F82H were close to those of conventional 9 Cr steels. The effects of ferromagnetism were estimated to be within a manageable level. The residual level of Nb in the IEA-F82H was evaluated to be at a level comparable to that required for reduced-activation material. The potential of the reduced activation martensitic alloys for application as a structural material for fusion reactors has been demonstrated. Exploring the limitation of the performance (including the resistance to irradiation damage), improvement of the properties, and the application to an ITER test blanket are seen to be the keys for the application of RAF/M steels to DEMO reactors.

References

- [1] Proceedings of the Workshop on Ferritic/Martensitic Steels, JAERI, Tokyo, Japan, 26–28 October 1992.
- [2] Proceedings of the IEA Working Group Meeting on Ferritic/Martensitic Steels (ORNL/M-4939), prepared by R.L. Klueh, Baden, Switzerland, 19–20 September 1995.
- [3] Proceedings of the IEA Working Group Meeting on Ferritic/Martensitic Steels (ORNL/M-5674), prepared by R.L. Klueh, Culham, UK, 24–25 October 1996.
- [4] Proceedings of the IEA Working Group Meeting on Ferritic/Martensitic Steels, JAERI, Tokyo, Japan, 3–4 November 1997.
- [5] Proceedings of the IEA Working Group Meeting on Ferritic/Martensitic Steels (ORNL/M-6627), prepared by R.L. Klueh, ECN, Petten, Netherlands, 1–2 October 1998.
- [6] Report of IEA Workshop on Reduced Activation Ferritic/Martensitic Steels (JAERI-Conf 2001-007), Tokyo, Japan, 2–3 November 2000.
- [7] N. Yamanouchi, *J. Nucl. Mater.* 191–194 (1992) 822.
- [8] K. Ehrlich, D.R. Harries, A. Möslang, Kernforschungszentrum Karlsruhe Report FZKA 5626, February 1997.
- [9] E. Daum, K. Ehrlich, M. Schirra, in: Proceedings of the Second Milestone Meeting of European Laboratories on the Development of Ferritic/Martensitic Steels for Fusion Technology, Kernforschungszentrum Karlsruhe Report FZKA 5848, May 1997.
- [10] V.K. Sikka, C.T. Ward, K.C. Thomas, in: A.K. Khare (Ed.), *Ferritic Steels for High-temperature Applications*, ASME, Metals Park, OH, 1983, p. 74.
- [11] E.V. van Osch, J.B.M. Baller, R. den Boef, J. Rensman, NRG, Petten Report 20023/99.26974/P, October 2000.
- [12] D.R. Harries, G.J. Butterworth, A. Hishinuma, F.W. Wiffen, *J. Nucl. Mater.* 191–194 (1992) 92.
- [13] E. Wakai, N. Hashimoto, Y. Miwa, J.P. Robertson, R.L. Klueh, K. Shiba, S. Jitsukawa, *J. Nucl. Mater.* 283–287 (2000) 799.
- [14] Y. Miwa, E. Wakai, K. Shiba, N. Hashimoto, J.P. Robertson, A.F. Rowcliffe, A. Hishinuma, *J. Nucl. Mater.* 283–287 (2000) 334.
- [15] E. Wakai, N. Hashimoto, J.P. Robertson, T. Sawai, A. Hishinuma, *J. Nucl. Mater.*, these Proceedings.
- [16] T. Sawai, E. Wakai, A. Naito, S. Jitsukawa, *J. Nucl. Mater.*, these Proceedings.